Indo. J. Chem. Sci. 12 (1) (2023)

Indonesian Journal of Chemical Science

http://journal.unnes.ac.id/sju/index.php/ijcs

New Ruthenium (II)Palladium (II) and Platinum (II) Complexes of Heterocyclic Organochalcogenide Ligands: Synthesis, Characterization, and Evaluation of Anticancer Activity Against Breast Cancer Cells

Hayat H. Abbas[a]✉,Mohammed J.B. Al-assadi[c], Majeed Y. Al-Luaibi[b]

[a,b]Department of Chemistry, College of Science, University of Basrah. Basrah, Iraq
[c]Al-Maaqal University. Basrah, Iraq

Article Info

Accepted : August 30, 2022

Approved : Jan 16, 2023

Published : May 2023

Keywords:
Selenomorpholine
Heterocyclic Ru (II)-complexes
Cytotoxicity in vitro
DNA binding activity

Abstract

This work aimed to synthesize, characterize of Ruthenium (II)Palladium (II) and Platinum (II) Complexes and to test the cytotoxic activity, against breast adenocarcinoma cell line (MCF-7) through conducting MTT assay and AO/EB dual staining-technique. Given our efforts ton toward the synthesis of coordination compounds with potential chemotherapeutic properties, we report In this manuscript, the synthesis, of seven new Ru(II), Pd(II), and, Pt(II) complexes with mono- and bidentate organo-chalcogenide ligands formulated $[M_2.\mu\text{-}2Cl(L)_4]Cl_2$ and $[M(L)_2]Cl_2$ of M=Ru(II) and Pd(II), Pt(II) respectively [where L= 4-phenylthiomorpholine-3,5-dione[I], 4-phenylselenomorpholine-3,5-dione[II] and O-chlorophenylselenomorpholine-3,5-dione[III]]ligands, which characterized by elemental analysis C.H.N, FTIR, UV-VIS, MSD-mass spectrometry, ^{1}H NMR, ^{13}C NMR, molar conductivity measurements and magnetic susceptibility. The preliminary cytotoxic activity of these compounds was evaluated against human breast carcinoma, MCF-7 and normal, breast cells, HBL-100 by a colorimetric viability assay based on enzymatic reduction of the MTT molecule to formazan when it is exposed to viable cells. To elucidate the apoptotic activity of the prepared compounds, the acridine orange/ethidium bromide (AO/EB) staining technique was conducted. The DNA binding activity of one of these ligands and it's corresponding Ru complex was confirmed by electronic spectroscopy studies. It was found at ligand(II) has stronger DBA than it's corresponding Ruthenium complex(V).

✉ Correspondence address:
[a,b]Department of Chemistry, College of Science, University of Basrah.Basrah,Iraq
[c]Al-Maaqal University. Basrah, Iraq
E-mail: hayat.hamza@uobasrah.edu.iq

Introduction

Chalcogen complexes possess a wide variety of activities against bacteria, fungi, and certain types of tumors. Some drugs show increased activity when administered as metal chelates and inhibit the growth of tumors. Metal complexes play an important role in inorganic medical chemistry and have significant potential for drug design(Ma et al., 2013) (Marina, 2013)and application because of their potential to bind DNA and cleave the duplex(Ejidike & Ajibade, 2016). Because of increasing chemoresistance, and some of its side effects, Cisplatin has limited use as an anticancer drug(Zeng et al., 2014)(Nemati et al., 2021). Therefore, there is a need for a novel Metallo -anticancer.

Generally, the reactivities of complexes were significantly affected by both their structures and the ligands involved. The activity of both catalytic and photoactive organometallic compounds is highly dependent not only on the metal and its oxidation state but also on the other coordinated ligands, the coordination number, and geometry. Selenium is a soft element with a high ability to coordinate with various transition metals of the second and third row(Alcolea et al., 2017). Selenium-containing molecules have attracted much attention as agents for the treatment of cancer, with some of these compounds showing good anticancer Activities(Chuai et al., 2021)(Du et al., 2014). Ligands containing sulfur coordinated to some metal ions, such as Pd (II), Pt (II), and Ru(II) showed a significant effect to treat cancer(Al-Harbi et al., 2020)(Ajibade et al., 2006)(Silva-Caldeira et al., 2021). It was interesting to use ligands containing selenium instead of sulfur, which give new drugs less toxicity. These types of complexes may induce a more strengthened chalcogen bond, than the corresponding compounds with sulfur and may make a significant effect on the biological surroundings in the biological studies. Among those complexes, Ru (II, III) complexes are of sustained interest in cancer research and become an alternative to platinum-based therapy(Trondl et al., 2014). Ruthenium complexes have attracted extensive attention as new anticancer drugs. Recently, many Pd (II) complexes with promising anticancer activity against tumor cell lines have been synthesized and reported elsewhere(Sharma et al., 2016)(Scattolin et al., 2021).

In this work, some new [Ru(II), Pd(II)& Pt(II)]-S/Se complexes have been prepared and their biological activities were explored using DNA-binding, MTT-assay, and AO/EB staining techniques. Cell apoptosis, which is associated with changes in the cell membrane, can be identified by using the dual Acridine orange/Ethidium Bromide(AO/EB)fluorescent staining method. This technique can also, be used to distinguish cells in different stages of the apoptosis process(Sathish Kumar et al., 2013). The AO/EB staining was conducted to test the apoptosis process in a human Breast cancer MCF-7 cell line treated with some of the prepared complexes namely Pd-OCl-Se, Ru-aniline-S, Ru-aniline-Se, Pt-aniline-Se, and Pt-OCl-Se.

Experimental

Materials

All the chemicals and solvents used were of analytical grade supplied from Aldrich, CHIYODA CORPORATION, Sigma-Aldrich, Fluka, Merck, BDH, HIMEDIA, and SCH. Potassium tetrachloropalladate (II)was supplied from Aldrich, and potassium tetra-chloroplatinate (II) was obtained from CHIYODA CORPORATION, chloroacetylchloride, sodium borohydride (NaBH4), and MTT stain were obtained from Sigma- Aldrich. Dichloromethane and Ruthenium (III) chloride hydrate was obtained from Fluka. Thin-layer chromatography (TLC) was carried out by using an aluminum sheet coated with silica gel 60F254 (Merck), iodine, and ultraviolet (UV) light was used for visualized TLC plates, NaCl, NaOH, and KOH from Merck product. Selenium Powder and Chloroform were purchased from BDH while dimethyl sulfoxide for UV spectroscopy was supplied from HIMEDIA, absolute ethanol absolute and ethyl acetate were obtained from SCH Normal (HBL-100) and cancer cell line (MCF-7) were collected from the IRAQ Biotech Cell Bank Unit in Basra and maintained in RPMI-1640 supplemented with 10% Fetal bovine,100 units/ml penicillin, and µg/mL Streptomycin. Cells were passaged using Trypsin-EDTA reseeded at 70% confluence twice to a third a week and incubated at 37℃ and 5% CO_2.

Instrumentation

Many techniques have been used for characterizing thiomorpholine and Selenomorpholine ligands and their Ru(II), Pd(II), and Pt(II) complexes. The melting points of all prepared compounds were determined by a Stuart melting point |SMP10|apparatus. FT-IR spectra were recorded using FT-IR-8400S Shimadzu Spectrophotometer in the range (4000-400)cm^{-1} in KBr disk. Elemental analysis for Carbon Hydrogen and Nitrogen was performed by using EuroFA-Vector-EA-3000 Elemental Analyzer Apparatus. ^{1}H and ^{13}C-NMR spectra were recorded on a Bruker DRX (500 MH_Z and 100 MH_Z respectively) using CD_3OD and

DMSO-d_6 as internal standards. The mass spectra were measured by the EI technique at 70 eV using Agilent Technologies 5973C spectrometer, while the UV-Vis spectra of ligands and their complexes were measured on a Shimadzu,1800 UV-VIS spectrophotometer. The molar_conductance of the prepared complexes in DMSO 25°C(10^{-5}) was conducted using Wiss-Techn. Warkstatten D812 Weilheim Mod.LBR/(Germany).

Synthesis of compounds

General procedure for the synthesis of 2-chloro-phenylacetamide:

N-phenyl-2-Chloro-N-(2-chloroacetyl) acetamide Ph-N($COCH_2Cl$)$_2$

A mixture of (4mmol) aniline and sodium carbonate (4.24g;4mmol) in 70 ml of acetone was stirred for 30 min. Chloroacetylchloride (6.5ml; 8mmol) was added dropwise. The reaction was left with stirring for two hours, then filtered and the acetone was removed under a vacuum. To the filtrate, 30 ml of distilled water was added(Khalib et al., n.d.). A white ppt. formed, dried then recrystallized from ethanol/water (ratio 80:20) mixture(Hassan et al., 2021), the product was obtained in 8o % yield. m.p. 127-129℃. The o-chlorophenyl-2-chloro-N-(2-chloroacetyl) acetamide o-ClPhN($COCH_2Cl$)$_2$ compound was prepared by the same procedure described, the product was obtained in 85 % yield m.p.71-73℃.

Synthesis of 4-Phenylthiomorpholine-3,5-dione (I)

To an aqueous solution of $Na_2S.3H_2O$ (0.32g;2.00mmol) a solution of N-phenyl-2-chloro-N-(2-chloroacetyl) acetamide (0.49g ;2.00mmol) in 20ml of ethanol was added under nitrogen atmosphere. After 30 min, a pale-yellow solution formed, and filtered,50 ml of H_2O was added and the resulting solution was extracted with three portions of CH_2Cl_2. The solvent evaporated to a minimum amount, a pale-yellow precipitate was collected, dried, and recrystallized from ethanol. A white solid was obtained in 83% yield, m. p. 172-174℃.

Synthesis of 4-phenylselenomorpholine-3,5-dione (II)

To a suspended solution of selenium powder (0.14g;1.8mmol) in 25ml of H_2O, a solution of $NaBH_4$ (0.118g; 3.1mmol) in 25 ml of H_2O was added under Argon atmosphere. A vigorous reaction occurs with the evolution of hydrogen gas. Selenium powder was consumed in less than 10 min. led to a formation of a colorless solution of NaHSe(Chuai et al., 2021). To the resulting solution was added a solution of N-phenyl-2-chloro-N-(2-chloroacetyl) acetamide (0.48g; 1.8mmol) in 20ml of ethanol was mixed under a nitrogen atmosphere. After 30 min, a violet solution was formed and filtered. To this solution, H_2O (50ml) was added, and the resulting solution was extracted with CH_2Cl_2. The solvent was evaporated, using a rotary evaporator, and a violate solid was obtained, collected by filtration, dried, and then Recrystallized from ethanol(Scattolin et al., 2021). The obtained violate solid was in 80% yield, m.p.210-212℃, The o-chlorophenylselenomorpholine-3,5-dione**(III)** (pale gray,80%yield, m.p123 ℃) compound was prepared by the same procedure described.

General procedure for the synthesis of Ruthenium complexes (IV/V):

The bivalent ruthenium complexes [Ru_2-μ-2Cl(aniline-S)$_4$] Cl_2 (IV) and [Ru_2-μ-2Cl(aniline-Se)$_4$]Cl_2 (V) were prepared according to literature method(de Melo et al., 2019), by mixing 25ml warm ethanolic solution (0.1mmol) of 4-phenyl(thio/seleno)morpholine-3,5-dione(I), (II) with ethanolic solution containing (0.1mmol, 0.0261g) of $RuCl_3.3H_2O$. The mixture was left under reflux for 6h with continuous stirring and then left overnight at room temperature. The mixture was filtered, dried, and washed with diethyl ether several times. The deep-red colored precipitate [Ru_2-μ-2Cl(aniline-S)$_4$]Cl_2 (IV) was obtained in 75% yield, m.p:247°C, While the shining-brown [Ru_2-μ-2Cl(aniline-Se)$_4$] Cl_2 (V)complex obtained in 68%, m.p.225-228°C,

General Consideration for Synthesis of Palladium complexes (VI/IX):

Initially, K_2PdCl_4 (0.12mmol;0.04g) dissolved in freshly prepared aqueous ethanol (absolute ethanol: water 1:1) at 37°C and (0.24mmol) of 4-phenylselenomorpholine-3,5-dione (II) / o-chlorophenylselenomorpholine-3,5-dione (III) ligand dissolved in (28ml absolute ethanol) were mixed in 1:2 molar ratio(Scattolin et al., 2021). The ligand solution was added dropwise to the metal compound solution with continuous stirring at room temperature. After 1.5h a light gray precipitate was formed apparently [Pd-aniline-Se)$_2$] Cl_2(VI). The

precipitate was filtered off and washed several times with (1:2) water: ethanol solution and kept overnight in a vacuum oven at room temperature for dryness. The lighting-brown Pd (II)complex was obtained in 77% yield, m.p.240-242°C. $[Pd(o\text{-}Cl\text{-}Se)_2]$ Cl_2 (IX) (lighting-brown, 80%yield, m.p201-203 °C) compound was prepared by the same procedure described.

General Consideration for Synthesis of Platinum complexes (VII/VIII):

In the line of study, (0.24mmol) of 4-(substituted) phenylselenomorpholine-3,5-dione (II/III) was dissolved in 20ml ethanol and then added dropwise, with continuous stirring at room temperature for 1h, to 10ml (water: absolute ethanol,1:1) solution containing (0.12mmol, 0.05g) of potassium- tetra chloroplatinate (K_2ptCl_4) at 37°C The former act as a monodentate ligand to give the corresponding heterocyclic Pt(II) complexes(Bellam et al., 2019). Analytical and spectroscopic data were in good conformity with the proposed structure of Pt(II) complexes $[Pt(L)_2]Cl_2$ as shown in Scheme 2, (where L=4-phenyselenomorpholine-3,5-dione) (II)] forming lighting-gray platinum complex(VII) obtained in 65% yield, m.p:268-270°C while the o-chlorophenylselenomorpholine-3,5-dione ligand(III)formed off-white platinum complex(VIII) which was collected in70% yield, m.p.254- 255°C.

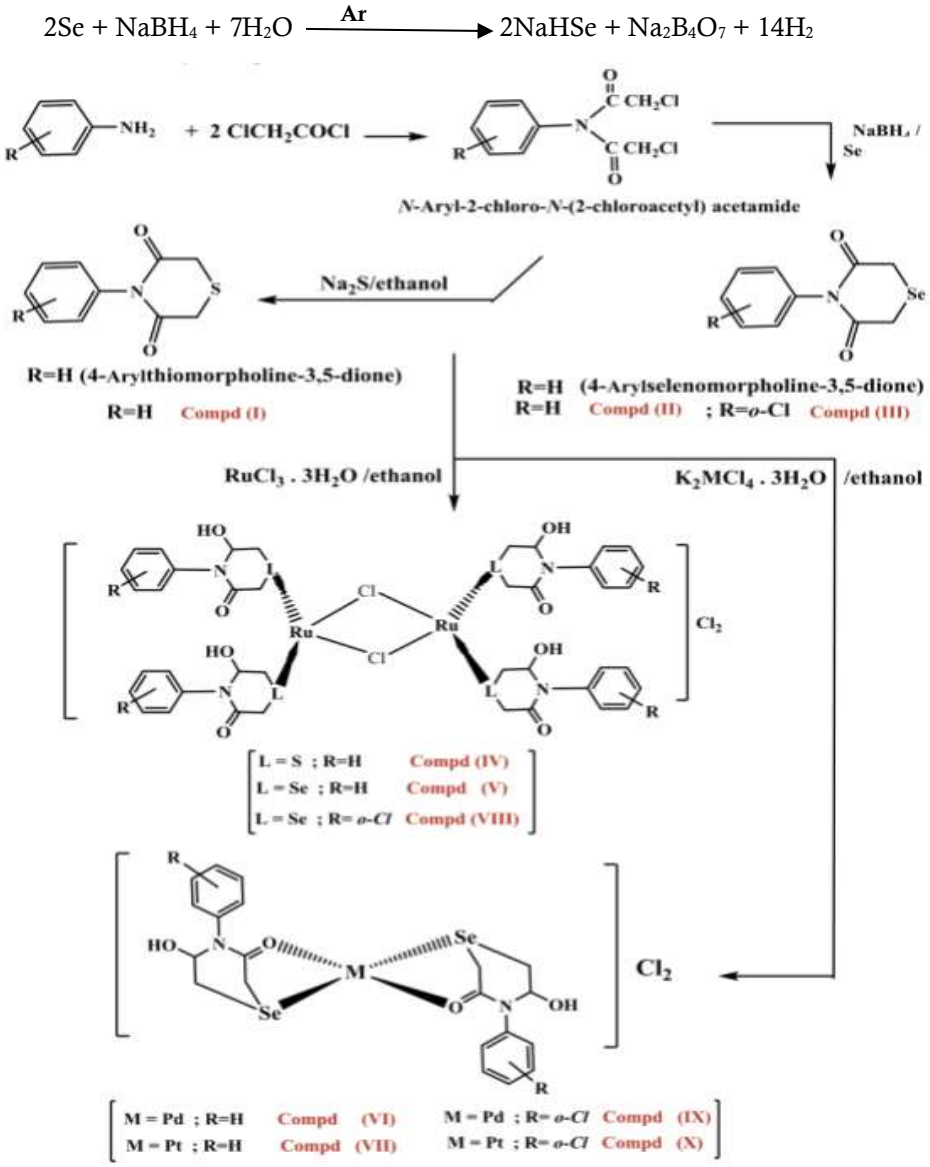

Scheme 1: Synthesis of chalcogenide compounds (I)-(X)

Biological Evaluation

- In vitro cytotoxicity test: Normal and cancer cell line (HBL 100 and MCF7), respectively.
- Positive control: DMSO
- Negative control: Serum-free media

cytotoxicity measurement using the MTT assay:

Evaluation of the anticancer activity of the prepared compounds can be achieved by the MTT assay. Thus, this technique is a colorimetric viability test based on enzymatic reduction of the MTT molecule to formazan when it is exposed to viable cells. The outcome of the reduction is a color change of the MTT molecule. Absorbance measurements relative to control determine the percentage of remaining viable cancer cells. The MTT assay is widely common in cytotoxicity studies due to its accuracy, rapidity, and relative simplicity. To determine the cytotoxic effect of three organo-chalcogenide compounds: 4- phenylthiomorpholine-3,5-dione(I) and 4-(substituted) phenylselenomorpholine-3,5-dione (II), (III) and their corresponding bivalent (ruthenium, palladium, and platinum) complexes (IV)-(X), the 3-(4,5-dimethylthiazole)-2,5-diphenyltetrazolium bromide (MTT) assay was conducted as the experimental cells were reseeded in 96-well micro assay culture plates(1x104) cells/well, then incubated at 37°C and 5% CO_2(Al-Ali & Jawad, 2021). After 24h or a confluent monolayer was achieved, cells were treated with the tested compounds(I)-(VIII), which dissolved in DMSO with one concentration (1000µg/ml). Suspended cell with complete media 10% reseeded in 96-well plate 100µl(1x104) cell/well, incubated at 37°C and 100% humidity 5%CO2. Untreated cells serve as a control group. Cell viability was measured after 72 hours of treatment by removing the medium, adding 28µl of 2mg/ml solution of MTT, and incubating the cells for 2h at 37°C. After removing the MTT solution, the crystals remaining in the wells were solubilized by the addition of 100 µl of DMSO followed by 37°C incubation for 15 min with shaking(Al-Shammari et al., 2019). The optical density of each well was measured on a microplate reader at 620nm (test wavelength). The assay was performed in triplicate to obtain mean values and the inhibition rate of cell growth i.e., the percentage of cytotoxicity, was calculated according to the following equation:

$$\text{Proliferation rate } (PR) = \frac{absorbance\ of\ compound-treated\ wells(B)}{well\ absorbence\ for\ a\ non-treated\ control\ group(A)}\ x100 \ldots\ldots\ldots\ldots (1)$$

Therefore, the inhibition rate (IR)was found as(Freshney, 2015):

$$\text{Inhibition rate (IR)} = 100 - \text{proliferation rate (PR)} \quad \ldots\ldots\ldots\ldots\ldots\ldots (2)$$

Apoptosis studies with AO/EB staining method

The morphological effect of the prepared thiomorpholine and selenomorpholine ligands and their corresponding bivalent complexes (ruthenium, Palladium, and Platinum) on MCF-7 cells were's detected by Dual acridine orange/ethidium bromide (AO/EB) fluorescent staining, visualized under fluorescent and light microscope(He et al., 2019). After a trypsinization process, cells are suspended by the RPMI1640 10% Fetal Bovine Serum medium, the suspended cells were cultured at 1 * 104 cells/well using special culture plates of 96 well, the plat wase then transferred into the incubator at 37°C and 5% CO2 humidity. The plates were incubated until the monolayer was formed. After 24 hours of incubation (a monolayer was formed), cell lines were treated with one concentrations of the above compounds (100µg/ ml) 100µl of that concentration put in each well of the culture plate with four replications for each one, then it was returned to the incubator at of temperature 37°C and 5% CO2 humidity and left for 72 hours. The experiment was replicated three times to ensure accurate results, this is as recommended (Abdel-Rahman et al., 2017).

DNA binding experiments

The human-DNA interactive studies of compound (II)and its corresponding bivalent ruthenium complex(V) were carried out in 5mmol/L Tris-HCl (121.14g/mol) and 50mmol/L NaCl (58.44g/mol) buffer (10mM, pH=7.2) which prepared in deionized water. 50 µM DNA stock in the buffer gave a ratio of UV

absorbance at 260 and 280nm of about >1.86 indicating that the used human DNA for absorption titration was sufficiently free from protein(Kaplanis et al., 2014). The concentration of DNA per nucleotide was determined by using the molar absorption coefficient $\mathcal{E}_{260}$=6600 M^{-1} cm^{-1}. The resulting DNA stock solution was kept at 4°C and used within 24h.A solutions of compound (II) and ruthenium complex(V) with constant concentration $3x10^{-4}$ M and $1.4x10^{-4}$ Respectively, was prepared in 10% DMSO with 90% Tris-HCl buffer. Upon addition of varying concentrations of DNA stock solution (20 -120) µM with 20 µM increments the resultant solutions were incubated at 25 °C for 15min before recording UV spectra(Shahabadi et al., 2009). The intrinsic binding constant (k_b) was determined by fitting the titration data into the following equation(Demirbas et al., 2009).

$$\frac{[DNA]}{\varepsilon_a-\varepsilon_f} = \frac{[DNA]}{\varepsilon_b-\varepsilon_f} + \frac{1}{K_b(\varepsilon_b-\varepsilon_f)} \quad \ldots\ldots\ldots\ldots\ldots (3)$$

ε_a, ε_f and ε_b are apparent, free, and bound compound extinction coefficients, respectively. ε_f was determined from a calibration curve of an isolated compound following Beer's law. ε_a matches the extinction coefficient of the particular absorption band at the specified DNA concentration (corresponding to A_{obs}/[complex], ε_b is equated to the extinction coefficient of fully bound compound to DNA. The plot of ([DNA])/(ε_a- ε_b) versus[DNA],produces a slop $1/(\varepsilon_a-\varepsilon_f)$ and a Y intercept of $1/(k_b(\varepsilon_b-\varepsilon_f)$ .The ratio of slop to the Y intercept is expected to be the intrinsic bonding constant (K_b).

Results and Discussion

^{1}H NMR spectroscopy provides a thorough structural information of the chalcogen ligand(I)(II)(III) and their corresponding bivalent (ruthenium, palladium and platinum) complexes (IV,V,VIII) (VI,IX) (VII,X)respectively. The obtained spectral data are in agreement with previous work(Al-Shammari et al., 2019)(Al-Rubaie et al., 2014). The proton NMR spectra were measured using a Brucker 1400 NMR instrument of 499.67 MHz frequency. DMSO-d_6 were employed as solvent at room temperature. The extracted chemical shift values, Figures 1, listed in Table 1. The main chemical shift ranged at 7.17 - 7.81 ppm, obviously due to the aromatic protons(Al-Rubaie et al., 2014)(Abdulnabi et al., 2021). The low field 9.70-9.72 ppm signals explore to possible tautomerism C_3-OH moiety and C_3=O carbonyl group as ketoenol form. Thus, it is supported by the appearance of high field signals at 3.49-3.31 ppm which might attributed to the (HO-C_3-H) proton, Scheme 2.

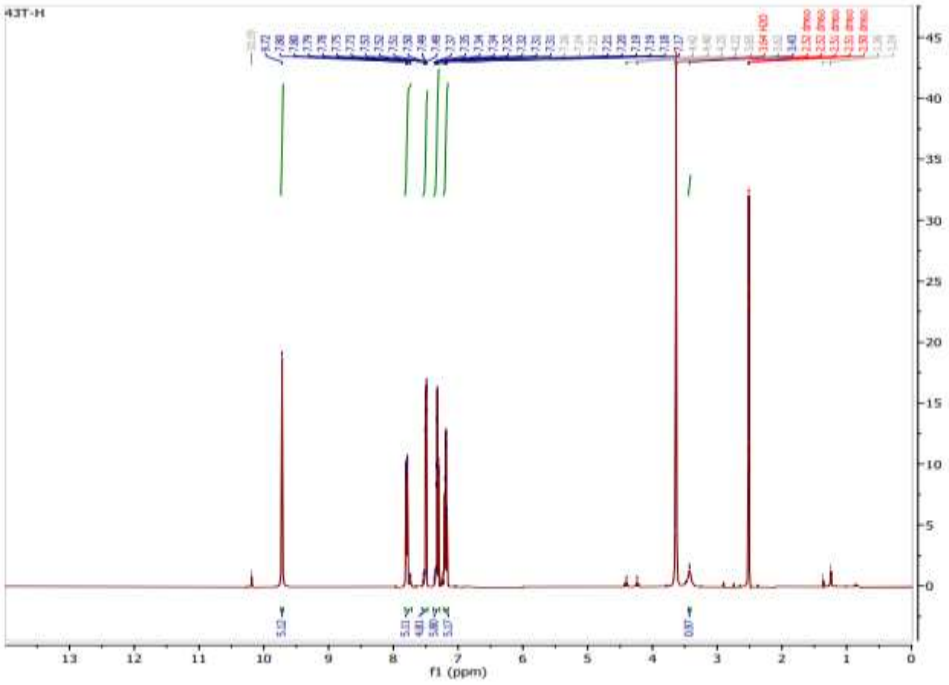

Figure 1. ^{1}H NMR of the Pt-OCl-Se complex (X) recorded in d^6 (DMSO) solution.

Table 1. ,1H NMR data for new chalcogen ligands and their corresponging metal-complexes

Compd. No.	Empirical formula	δ (ppm)
I	aniline-S	3.32(1H$_3$,s); 3.62(4H$_1$,s); 7.07-7.04(1H$_7$,t,Ar) ; 7.35-7.31(1H$_6$, 1H$_8$,t,Ar) ; 7.60-7.59(1H$_5$, 1H$_9$,d,Ar);10.19(OH,s)
IV	Ru-aniline-S	3.51(1H$_3$,s); 3.52(4H$_1$,s); 7.08-7.05(1H$_7$,t,Ar) ; 7.33-7.30(1H$_6$, 1H$_8$,t,Ar) ; 7.61-7.59(1H$_5$, 1H$_9$,d,Ar);10.21(OH,s)
II	aniline-Se	3.36(1H$_3$,s); 3.65(4H$_1$,s); 7.10-7.04(1H$_7$,t ,Ar); 7.34-7.30(1H5, 1H8, t, Ar); 7.59-7.58(1H$_5$, 1H$_9$, d, Ar); 10.15(OH ,s) .
V	Ru-aniline-Se	3.54(1H$_3$,s); 3.65(4H$_1$,s); 7.06-7.04(1H$_7$,t,Ar); 7.33-7.30(1H$_6$, 1H8 ,t,Ar); 7.63-7.58(1H$_5$, 1H$_9$,d,Ar); 10.18(OH,s)
VI	Pd-aniline-Se	3.54(1H$_3$,s); 3.54(4H$_1$,s); 7.08-7.05(1H$_7$, t ,Ar); 7.33-7.30(1H$_6$, 1H8 ,t,Ar) 7.59-7.57(1H$_5$, 1H$_9$,d,Ar); 10.16(OH,s)
VII	Pt-aniline-Se	3.54(1H$_3$,s) ;3.56(4H$_1$,s) ;7.10-7.04(1H$_7$,t ,Ar); 7.35-7.30(1H$_6$, 1H$_8$,t,Ar) ; ; 7.59-7.58(1H$_5$ 1H$_9$,d,Ar); 10.17(OH ,s) .
III	O-Cl-Se	3.31(1H$_3$,s) ; 3.63(4H$_1$,s) ;7.21 -7.17(1H$_7$,t , Ar) 7.34-7.31(1H$_8$,t,Ar) ; 7.51-7.49(1H$_9$,d,Ar) 7.81-7.79(1H$_6$,d,Ar).9.70(OH.s)
VIII	Ru+O-Cl-Se	3.49(1H$_3$,s); 3.63(4H$_1$,s); 7.24-7.17(1H$_7$, t ,Ar); 7.34-7.31(1H$_8$, t, Ar); 7.50-7.39(1H$_9$,d,Ar); 7.80-7.78(1H$_6$,d,Ar) ; 9.72(OH,s)
IX	Pd+O-Cl-Se	3.43(1H$_3$,s); 3.47(4H$_1$,s); 7.21-7.18(1H$_7$, t ,Ar); 7.34-7.33(1H$_8$, t, Ar); 7.51-7.49(1H$_9$,d,Ar); 7.80-7.87(1H$_6$,d,Ar) ; 9.71(OH,s)
X	Pt+O-Cl-Se	3.43(1H$_3$,s); 3.65(4H$_1$,s); 7.21-7.17(1H$_7$, t ,Ar); 7.35-7.31(1H$_8$, t, Ar); 7.53-7.49(1H$_9$, d,Ar); 7.80-7.73(1H$_6$,d,Ar) ; 9.72(OH,s)

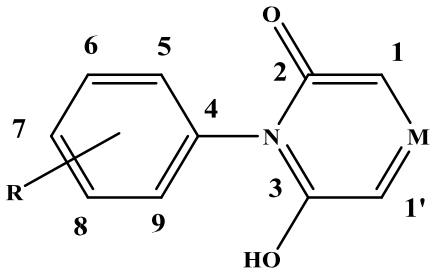

M=S or Se ; R=H or chloride

3-hydroxy-4-(substuted) phenylchalcogenomorpholine-2-one

Scheme 2. The suggested structure for the prepared ligands**.**

Infrared spectroscopy

The physical properties and analytical data of the prepared organo-chalcogenides ligands and their corresponding metal complexes are listed in Table 2. While their chemical structures were identified by FT-IR analysis using the previous analytical data available in the literature (Bhasin et al., 2003)(Mehta et al., 2010)**.** The FT-IR bands which belong to the main functional groups of the prepared compounds, appeared sharp and characteristic bands, as summarized in Table 3.

All chalcogen ligands(I)-(III) and bivalent metal complexes (IV)-(X)show a medium intensity bands at(1647-1654)cm^{-1} and (1647-1681)cm^{-1} respectively, due to **υ**(C=O) stretching frequency .The high intensity bands at (1531-1554) cm^{-1} and (1531-1589) cm^{-1} respectively, due to unsymmetrical stretching vibration of **υ**(C=C),

while(Se-C) stretching vibrations were observed around (493-497) $cm^{-1}$and (447-493) cm^{-1},respectively(Al-Harbi et al., 2020)(Ajibade et al., 2006) and (S-C) stretching vibrations were observed around (752) and (756) cm^{-1} ,respectively .The stretching vibrations of C- H_{al} and C-H_{ar} bands were found at expected regions(Bhasin et al., 2003)(Andrade & Silva, 2008).

Table 2. Physical properties and analytical data for the synthesized ligands.

Comp. No.	Empirical formula	formula wt	M.P (°C)	Yield %	Elemential analysis calculated(found) C%	H%	N%
I	$C_{10}H_9NO_2S$	207.06	172—174	83	57.95(57.79)	4.34(4.32)	6.76(6.74)
II	$C_{10}H_9NO_2Se$	253.96	210-212	80	47.25(47.22)	3.54(3.59)	5.51(5.49)
III	o-$ClC_{10}H_8NO_2Se$	289.41	123	80	41.46(41.70)	2.76(2.75)	4.83(4.80)
IV	$[Ru_2\text{-}2\mu\text{-}Cl(C_{10}H_9NO_2S)_4]Cl_2$	1170.4	247	67	41.01(41.34)	3.07(3.33)	4.78(5.02)
V	$Ru_2\text{-}2\mu\text{-}Cl(C_{10}H_9NO_2Se)_4]Cl_2$	1357.9	212-215	78	-	-	-
VI	$[Pd(C_{10}H_9NO_2Se)_2]Cl_2$	684.32	240-242	82	-	-	-
VII	$[Pt(C_{10}H_9NO_2Se)_2]Cl_2$	773.02	268-270	77	31.04(31.38)	2.32(2.47)	3.62(3.92)
VIII	Ru_2-2u-$Cl(o\text{-}C_{10}H_8NO_2Se)_4]Cl_2$	1499.78	202-205	68	-	-	-
IX	$[Pd(C_{10}H_8NO_2Se)_2]Cl_2$	755.22	203-205	65	31.77(31.08)	2.38(2.65)	3.70(3.25)
X	$[Pt(C_{10}H_8NO_2Se)_2]Cl_2$	773.02	254-255	66	28.44(30.00)	2.13(2.31)	3.32(3.45)

Table 3. Infrared Spectra for main bands(cm^{-1}) Uv-Visible Spectra(nm).

Comp. No.	Empirical formula	formula wt	M.P (°C)	Yield %	Elemential analysis calculated(found) C%	H%	N%
I	$C_{10}H_9NO_2S$	207.06	172-174	83	57.95(57.79)	4.34(4.32)	6.76(6.74)
II	$C_{10}H_9NO_2Se$	253.96	210-212	80	47.25(47.22)	3.54(3.59)	5.51(5.49)
III	o-$ClC_{10}H_8NO_2Se$	289.41	123	80	41.46(41.70)	2.76(2.75)	4.83(4.80)
IV	$[Ru_2\text{-}2\mu\text{-}Cl(C_{10}H_9NO_2S)_4]Cl_2$	1170.4	247	67	41.01(41.34)	3.07(3.33)	4.78(5.02)
V	$[Ru_2\text{-}2\mu\text{-}Cl(C_{10}H_9NO_2Se)_4]Cl_2$	1357.9	212-215	78	-	-	-
VI	$[Pd(C_{10}H_9NO_2Se)_2]Cl_2$	684.32	240-242	82	-	-	-
VII	$[Pt(C_{10}H_9NO_2Se)_2]Cl_2$	773.02	268-270	77	31.04(31.38)	2.32(2.47)	3.62(3.92)
VIII	$[Ru_2$-2u-$Cl(o\text{-}C_{10}H_8NO_2Se)_4]Cl_2$	1499.78	202-205	68	-	-	-
IX	$[Pd(C_{10}H_8NO_2Se)_2]Cl_2$	755.22	203-205	65	31.77(31.08)	2.38(2.65)	3.70(3.25)
X	$[Pt(C_{10}H_8NO_2Se)_2]Cl_2$	773.02	254-255	66	28.44(30.00)	2.13(2.31)	3.32(3.45)

Mass Spectrum

The mass spectra of some synthesized bivalent complexes (ruthenium, Palladium and Platinum) (IV, V); (IX) and (VII) respectively, were carried out at 30, 230, and 300 °C at 70eV. The Fragmentation of the compounds show common features in the mass spectra. All compounds show the absence of molecular ion, which may be attributed to the dissociation of the parent compound need using lower than 70eV (al-luaibi majeed y, 2013)(asmaa b.sabti, 2020). The mass spectra of compound (IX) Figure 2, shows a peak at m/z=(417) which is corresponding to $[C_{10}H_{11}CI_2NOPdSe]^+$ m/z=(368.01) which is corresponding to $[C_9H_9CINOPdSe\ ]^+$ ion and a peak at m/z=213) which is corresponding to $[C_{10}\ H_{12}CINO_2\ ]^+$ ion. This compound shows a base peak at m/z=(126.9) corresponding to the loss of $[C_6H_5CIN]^+$ ion.

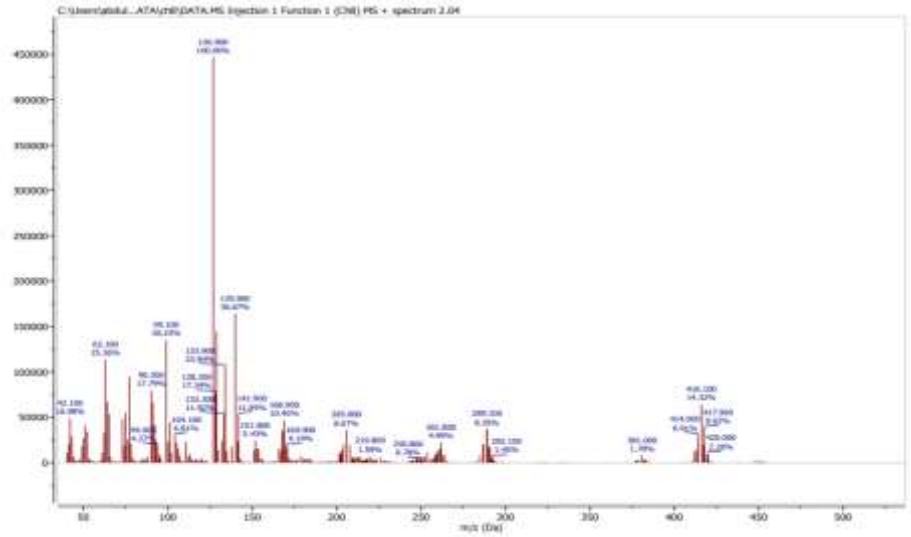

Figure 2. EI Mass spectrum for compound (IX)

The mass spectra of compound (IV) shows a peak at m/z=(207.1) which is corresponding to $[C_{10}\ H_9\ NO_2\ S\ ]^+$ ion, a base peak at m/z=(93) which is corresponding to $[C_6\ H_7N]^+$ ion and a peak at m/z=(78) which is corresponding to $[C_6\ H_6\ ]^+$ ion. This ion gave four fragments $[C_5\ H_6]^+$, $[C_4\ H_8]^+$, $[C_4\ H_6]^+$ and $[C_3\ H_6]^+$,which recorded with other organic fragment can be extracted from the EI mass spectra of compound (lV).

The mass spectra of compound (V) shows a peak at m/z=(254) which is corresponding to $[C_{10}\ H_9\ NO_2\ Se\ ]^+$ ion, a base peak at m/z=(93) which is corresponding to $[C_6\ H_7N]^+$ ion and a peak at m/z=(78) which is corresponding to $[C_6\ H_6\ ]^+$ ion. This ion gave four fragments $[C_5\ H_6]^+$, $[C_4\ H_8]^+$, $[C_4\ H_6]^+$ and $[C_3\ H_6]^+$, which recorded with other organic fragments can be extracted from the EI mass spectra of compound (V).

The mass spectra of compound (VII) shows a peak at m/z=(255) which is corresponding to $[C_{10}\ H_{11}\ NO_2\ Se\ ]^+$ ion, also gave the fragment at m/z=(346) that can be attributed to $[C_8H_9NO_2\ Pt\ ]^+$ ion and a base peak at m/z=(93.1) which is corresponding to $[C_6\ H_7N]^+$ ion. In the second step a loss of Se gave a peak at m/z=79 and other organic fragments can be extracted from the EI mass spectra of compound (VII). These peaks support our study while the structures of synthesized compounds are correct.

In vitro Cytotoxicity assay Methyl-thiazole-tetrazolium (MTT) test

The cytotoxic activities of the three ligands(I-III) and their corresponding bivalent (ruthenium, Palladium and Platinum) complexes were examined on cultured human Breast cancer MCF-7 cell lines for 24 hrs. onto the medium containing the prepared complexes of 1000µg/mL concentration.The cytotoxicity of these tested compounds was evaluated by the MTT-assay as the optical absorbance were measured at 620nm. Normal healthy cells, HBL100 Cell lines were employed to test the target-selection potency of the studied complexes. The obtained results are listed in Table 4 and shown in Figures (4). These figures (4A,4B) show the vitality of the cell lines. breast cancer cell line (MCF-7) and normal breast cell line (HBL-100) respectively, were exposed to one concentration (1000)µg/mL, of each one of the three ligands(I)-(III) and their corresponding bivalent (ruthenium, Palladium and Platinum) complexes. This concentration causes growth inhibition of normal and

human MCF-7 breast cancer cell. The obtained results revealed that Pd and Pt complexes exhibit more activities than their corresponding Ru complexes. Thus, the complex Pt-OCl-Se(X) has cell viability percentage of the prepared compounds, and the lower value, 27.33%, in belongs to the Pt-aniline-Se 20.73% i.e. the lowest rate of, vital percentage ultimately, it is the most effective species among complex (VII), Whereas their Pd and Ru complexes corresponding showed less cell viability percentages 29%; Pd-OCl-Se(IX), and 33% for $[Ru_2.\mu\text{-}2Cl(aniline\text{-}Se)_2\,Cl_2]$(V). The data, also, explore that complexes containing Se are more effective than those bearing S-atom, Table 4. However, these Ru and Pt complexes revealed a moderate selection capability as the HBL-100 cell lines testes reflect, Figure 3B and Table 4.

Table 4. in vitro cytotoxicity of the prepared compounds

Item No.	Compound	Absorbance	Cell viability MCT-7 %	Toxicity HBL-100 %	AO/EB %
X	Pt-OCl-Se	0.0935	20.73	41.07	55
VII	Pt-aniline-Se	0.12325	27.33	43.27	60
IX	Pd-OCl-Se	0.13525	29.99	46.24	65
II	aniline-Se	0.o665	32.06	30.91	70
V	Ru-aniline-Se	0.14775	33.40	28.86	85-90
III	OCl-Se	0.0735	35.43	-	90-95
IV	Ru-aniline-S	0.159	35.95	27.08	50

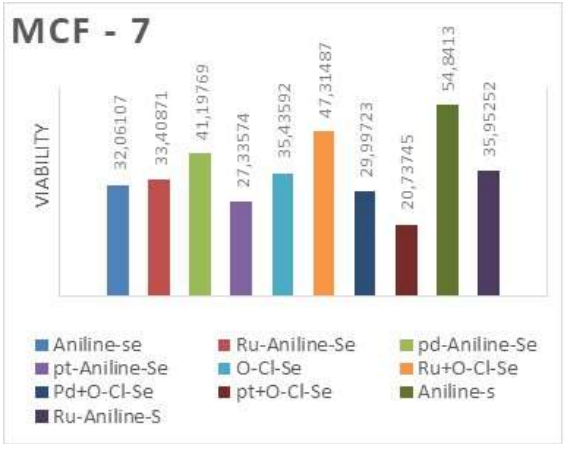

Figure 3A.
Chalcogenides ligands and complexes (1000 µg/mL)

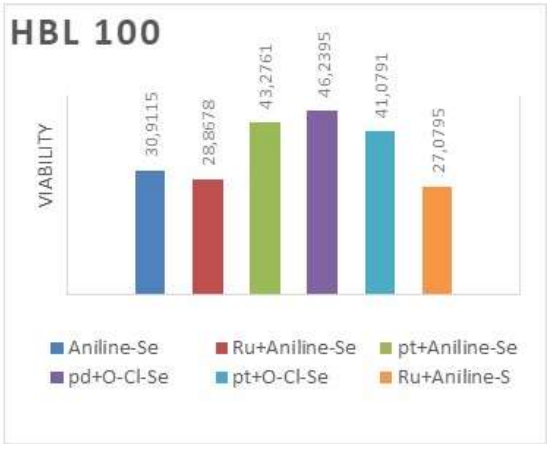

Figure 3B.
Chalcogenides ligands and complexes (1000 µg/mL)

Figure 3. percentage of cell viability in the cell line of:
A-breast cancer type (MCF-7) vs one concentration (1000) µg/mL for each one of the ten prepared compounds (I)-(X), 4- phenylthiomorpholine ligands (I), 4-(substituted)phenylSelenomorpholine ligands (II)-(III) and of their corresponding metal complexes (IV)-(X). B-normal breast cell line (HBL-100) vs one concentration (1000)µg/mL for each one of the prepared compounds [ligand (II) and complexes (IV), (V), (VII), (IX), and (X)] added to the medium.

The following sequence can be established to compare the effectiveness of the prepared compounds against the breast cancer cell line (MCF-7) referring to Table 4.

- aniline-Se > OCl-Se > aniline-S
- Pt-aniline-Se > aniline-Se > Ru-aniline-Se > Ru-aniline-S
- Pt-OCl-Se > Pd-OCl-Se > OCl-Se
- Pt-OCl-Se > Pt-aniline-Se > aniline-Se > OCl-Se

While the following sequence shows the influence of these compounds on the normal healthy HBL-100 cell line: Pt-aniline-Se > Pt-OCl-Se > aniline-Se > Ru-aniline-Se > Ru-aniline-S

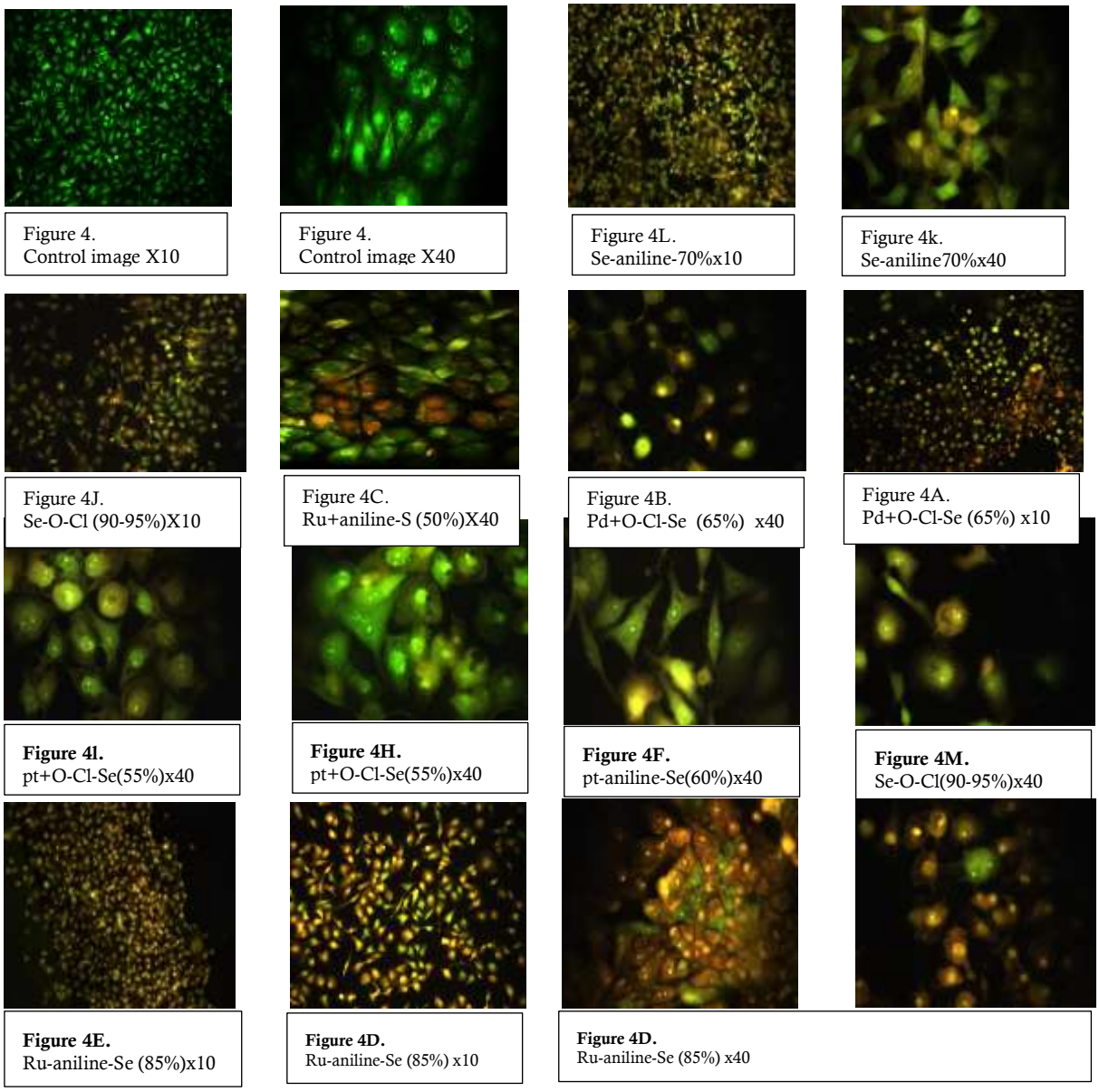

Figure 4. MCF-7 cell line dye AO/EB stain.

Figure 4. untreated cells look unaffected forming a monolayer strain green with AO/EB at magnification 10X and 40X. Figure 4D. and 4E. revealed the late-stage apoptotic cells due to the Ru-aniline-Se complex activity, Figure 4A. and 4B. Cells treated with compound (IX)Pd-OCl-Se, Figure 4C. with enlarged cell volume, this is related to the Ru-aniline-S complex, Figure 4F. and 4G. linked to the effect of Pt-aniline-Se, Figure 4H. and 4I. the early-stage due to the Pt-OCl-Se activity, Figure 4M. and 4J. related to the OCl-Se compound, appear affected as colored in yellow AO/EB at magnification 10X. Cells treated with compound (VIII); loss of normal characteristics refers to one of the early stages of cell death, AO/EB at magnification 40X. (d) and (e) images of (b) and (c) at magnification 40X.

AO/EB staining and programmed cell death

After the application of the prepared complexes, the MCF-7 cells were labeled by the AO/EB for 24hrs, and the dual staining was examined under a fluorescent microscope. Figure 4 (A to M) represents the obtained morphological images of the apoptotic cells while the extracted percentage are listed in Table 5. Those figures explored the apoptotic different stages. Thus, it can be noticed that Figures 4D and 4E revealed the late-stage

apoptotic cells due to the Ru-aniline-Se complex activity as indicated by the asymmetrically localized orange nuclear EB staining (85% - 90%). This pattern, also, can be observed in Figures 4A and 4B of Pd-OCl-Se but with less extent (65%). The orange nuclear EB staining, also, posed in Figure 4C, with enlarged cell volume, is related to the Ru-aniline-S complex action (50%). The early-stage apoptotic process can be detected in Figures 4F and 4G where the cells appear in marked crescent-shape and granular yellow-green AO nuclear staining. Thus, it is linked to the effect of Pt-aniline-Se (60%). Figures 4H and 4I explored the early stage due to the Pt-OCl-Se activity (55%) as indicated by the appearance of swollen-shape, and widely separated apoptotic cellular nuclei, with yellow-green fluorescence. According to the following order:

- OCl-Se(Hayat H. Abbas et al., 2022) (90-95 %) > Pd-OCl-Se (65%) > Pt-OCl-Se (55%) obviously, one can conclude that ligand OCl-Se is more effective on MCF-7 cells than its corresponding complexes of both Pd and Pt metals.

Comparing the activities of aniline-Se Figures 4K and 4L to its own Ru and Pt complexes suggest the following sequence:

- Ru-aniline-Se (85 – 90%) > aniline-Se (70%) > Pt-aniline-Se (60%). Which revealed that the Ru-aniline-Se complex is more effective and with promising cytotoxic compound versus breast cancer.
- Although, there are mismatches between the MTT-assays and the AO/EB staining results, but it has been proved that the latter technique is more accurate and distinguishable(Liu et al., 2015).

DNA -binding

Absorption studies: The binding of a prepared ligand(II) and their corresponding bivalent Ru-complex(V) to the helix has been characterized through the measurement of absorbance and the significant shift of maxima as a function of the added amount of DNA(20-120)μM to a fixed ligand's and complex's concentration ($3.0x10^{-4}$ μM) and ($1.4x10^{-4}$ μM) respectively. For ligand(II) and Ru- complex(v), Figure 5, the broadband at 260nm was monitored as it has been noticed that increase in the amount of DNA led to decreasing in molar absorptivity beside an (8-10)nm red shift i.e a hypochromic shift indicating intercalative interaction of ligand(II) and complex(V) with DNA. The intrinsic binding constant of the two compounds was found to be k_b=($3.6x10^6$ M^{-1} and ($1.25x10^6$ M^{-1}) respectively, as shown in Figure 5 (inset) suggesting a moderate intercalative interaction, compared to classical intercalators (k_b ~ 10^6 M^{-1}) as a function of added DNA. The isosbestic point at 290nm confirms the bonding of both compounds with DNA(Kulkarni & Revankar, 2011)(Shahabadi et al., 2011).

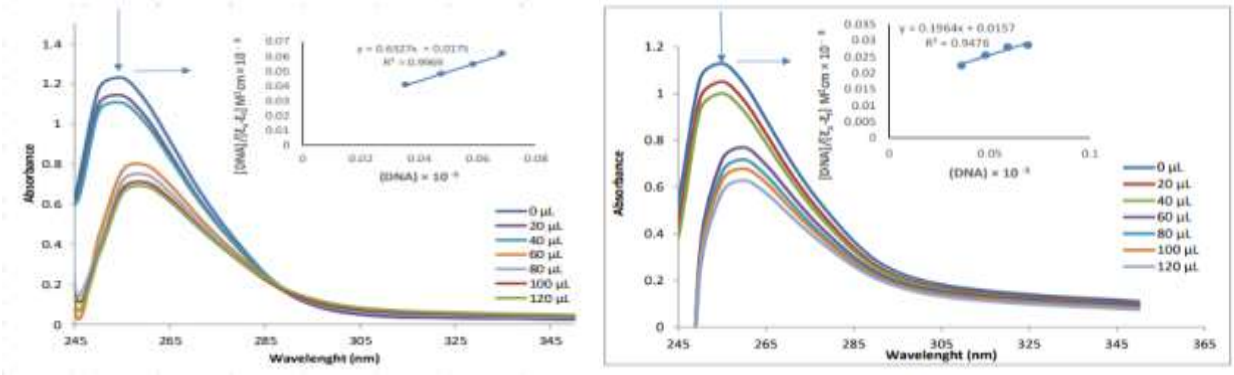

A- **B-**

Figure 5. Overlay UV-Vis Spectra of (**A)** 4-phenylselenomorpholine-3,5-dione(II), ligand and (**B)** [$Ru_{2\text{-}2}$μ-Cl(4-phenylselenomorpholine)$_4$]Cl_2, complex(V), in the absence and presence of increasing amounts of human-DNA. Arrow indicates that absorbance changes upon increasing DNA concentrations. Inset: Plot of [DNA]/(ε_a-ε_f)$x10^{-8}$ vs [DNA]$x10^{-5}$ and the linear fit for the titration.

Conclusion

The results of absorption studies show that the absorption intensity decreased (hypsochromism) evidently after the addition of DNA, which indicates that the interaction between DNA and ligand (II) and Ru-complex(V) occurred. Thus,these intrinsic binding constants(k_b=3.6x10^6 M^{-1} and 1.25x10^6 M^{-1}) respectively, are roughly comparable to other intercalators interaction(Uma Maheswari et al., 2005). According to the toxicity of the three ligands and their corresponding Pd, Ru, and Pt- chalcogenides/Se complexes measured through the MTT-assay to both normal and cancerous lines, they have no selective or directed action on cancerous cell. Nevertheless, this method does not provide any information regarding the cell death mechanism, the phase in the cell cycle that is affected by the drug, and its possible biological target.The dual AO/EB fluorescent staining method was conducted to diagnose stages of programmed cell death. It can be concluded that the low viability percentage of compounds (II),(III), and some Pd, Ru, and Pt- chalcogenides/Se complexes Figure 4 besides the cytofluorimetric inconclusive results may indicate that these prepared compounds may have the ability of cell-growth inhibition and potentially promising anticancer drug for breast cancer, and the Ru-aniline-Se complex might be the most expectant one. More studies need to be subjected to confirm this conclusion.

References

Abdel-Rahman, L. H., El-Khatib, R. M., Nassr, L. A. E., & Abu-Dief, A. M. (2017). DNA binding ability mode, spectroscopic studies, hydrophobicity, and in vitro antibacterial evaluation of some new Fe (II) complexes bearing ONO donors amino acid Schiff bases. *Arabian Journal of Chemistry*, *10*, S1835–S1846.

Abdulnabi, Z. A., Al-doghachi, F. A. J., & Abdulsahib, H. T. (2021). Synthesis, Characterization and Thermogravimetric Study of Some Metal Complexes of Selenazone Ligand Nanoparticles Analogue of Dithizone. *Indonesian Journal of Chemistry*, 1231–1243.

Ajibade, P. A., Kolawole, G. A., O'brien, P., & Helliwell, M. (2006). Synthesis and characterization of Ni (II), Pd (II) and Pt (II) complexes of 2, 4-diamino-5-(3, 4, 5-trimethoxybenzyl) pyrimidine complexes. *Journal of Coordination Chemistry*, *59*(14), 1621–1628.

Al-Ali, A. A. A., & Jawad, R. K. (2021). Cerium Oxide Nanoparticles Ceo2np and Retinoic Acid Trigger Cytotoxicity and Apoptosis Pathway in Human Breast Cell Lines. *Annals of the Romanian Society for Cell Biology*, 8448–8477.

Alcolea, V., Garnica, P., Palop, J. A., Sanmartín, C., González-Peñas, E., Durán, A., & Lizarraga, E. (2017). Antitumoural sulphur and selenium heteroaryl compounds: thermal characterization and stability evaluation. *Molecules*, *22*(8), 1314.

Al-Harbi, S. A., Al-Saidi, H. M., Debbabi, K. F., Allehyani, E. S., Alqorashi, A. A., & Emara, A. A. A. (2020). Design and anti-tumor evaluation of new platinum (II) and copper (II) complexes of nitrogen compounds containing selenium moieties. *Journal of Saudi Chemical Society*, *24*(12), 982–995.

al-luaibi majeed y. (2013). *some new organotellurium compound of chalcones, ferrocenyl chalcones and tetralene*.

Al-Rubaie, A. Z., Al-Jadaan, S. A. S., Muslim, S. K., Ali, E. T., Al-Fadal, S. A. M., Suad, A. K., Al-Salman, H. N. K., & Saeed, E. A. (2014). Synthesis and Biological Studies of Some Sulfur, Selenium and Tellurium Organic Compounds Based on Diethanolamine. *International Journal of Scientific Research*, *5*, 145–149.

Al-Shammari, A. M., Al-Esmaeel, W. N., al Ali, A. A. A., Hassan, A. A., & Ahmed, A. A. (2019). Enhancement of oncolytic activity of newcastle disease virus through combination with retinoic acid against digestive system malignancies. *Molecular Therapy*, *27*(4), 126–127.

Andrade, L. H., & Silva, A. v. (2008). First chemoenzymatic synthesis of organoselenium amines and amides. *Tetrahedron: Asymmetry*, *19*(10), 1175–1181.

asmaa b.sabti. (2020). *characterization and biological study of some new organotellurium compounds based on pyrazole and thiadiazole derivatives*.

Bellam, R., Jaganyi, D., Mambanda, A., Robinson, R., & BalaKumaran, M. D. (2019). Seven membered chelate Pt (ii) complexes with 2, 3-di (2-pyridyl) quinoxaline ligands: studies of substitution kinetics by sulfur donor nucleophiles, interactions with CT-DNA, BSA and in vitro cytotoxicity activities. *RSC Advances*, *9*(55), 31877–31894.

Bhasin, K. K., Jain, V. K., Kumar, H., Sharma, S., Mehta, S. K., & Singh, J. (2003). Preparation and characterization of methyl substituted 2, 2′-dipyridyl diselenides, 2, 2′-dipyridyl ditellurides, and their derivatives. *Synthetic Communications*, *33*(6), 977–988.

Chuai, H., Zhang, S.-Q., Bai, H., Li, J., Wang, Y., Sun, J., Wen, E., Zhang, J., & Xin, M. (2021). Small molecule selenium-containing compounds: Recent development and therapeutic applications. *European Journal of Medicinal Chemistry*, *223*, 113621.

de Melo, A. C. C., Santana, J. M., Nunes, K. J. R. C., Rodrigues, B. L., Castilho, N., Gabriel, P., Moraes, A. H., Marques, M. de A., de Oliveira, G. A. P., & de Souza, Í. P. (2019). New heteroleptic ruthenium (II) complexes with sulfamethoxypyridazine and diimines as potential antitumor agents. *Molecules*, *24*(11), 2154.

Demirbas, A., Sahin, D., Demirbas, N., & Karaoglu, S. A. (2009). Synthesis of some new 1, 3, 4-thiadiazol-2-ylmethyl-1, 2, 4-triazole derivatives and investigation of their antimicrobial activities. *European Journal of Medicinal Chemistry*, *44*(7), 2896–2903.

Du, P., Viswanathan, U. M., Xu, Z., Ebrahimnejad, H., Hanf, B., Burkholz, T., Schneider, M., Bernhardt, I., Kirsch, G., & Jacob, C. (2014). Synthesis of amphiphilic seleninic acid derivatives with considerable activity against cellular membranes and certain pathogenic microbes. *Journal of Hazardous Materials*, *269*, 74–82.

Ejidike, I. P., & Ajibade, P. A. (2016). Ruthenium (III) complexes of heterocyclic tridentate (ONN) Schiff base: Synthesis, characterization and its biological properties as an antiradical and antiproliferative agent. *International Journal of Molecular Sciences*, *17*(1), 60.

Freshney, R. I. (2015). *Culture of animal cells: a manual of basic technique and specialized applications*. John Wiley & Sons.

Hassan, A. F., Abdalwahed, A. T., Al-Luaibi, M. Y., & Aljadaan, S. A. (2021). Synthesis, Characterization and Thermal Study of some new Organochalcogenide compounds containing arylamide group. *Egyptian Journal of Chemistry*, *64*(9), 1–2.

Hayat H. Abbas, Majeed Y. Al-Luaibi, & and Mohammed J.B. Al-assadi. (2022). *, New Heterocyclic Organo-chalcogenide Compounds : Synthesis, Physicochemical Characterization and Evaluation of Anticancer Activity Against Breast Cancer Cells*.

He, M., Du, F., Zhang, W.-Y., Yi, Q.-Y., Wang, Y.-J., Yin, H., Bai, L., Gu, Y.-Y., & Liu, Y.-J. (2019). Photoinduced anticancer effect evaluation of ruthenium (II) polypyridyl complexes toward human lung cancer A549 cells. *Polyhedron*, *165*, 97–110.

Kaplanis, M., Stamatakis, G., Papakonstantinou, V. D., Paravatou-Petsotas, M., Demopoulos, C. A., & Mitsopoulou, C. A. (2014). Re (I) tricarbonyl complex of 1, 10-phenanthroline-5, 6-dione: DNA binding, cytotoxicity, anti-inflammatory and anti-coagulant effects towards platelet activating factor. *Journal of Inorganic Biochemistry*, *135*, 1–9.

Khalib, A. A. K., Al-Hazam, H. A. J., & Hassan, A. F. (n.d.). Inhibition of Carbon Steel Corrosion by Some New Organic 2-Hydroselenoacetamide Derivatives in HCl Medium. *Indonesian Journal of Chemistry*.

Kulkarni, N. v, & Revankar, V. K. (2011). Synthesis, antimicrobial screening, and DNA-binding/cleavage of new pyrazole-based binuclear CoII, NiII, CuII, and ZnII complexes. *Journal of Coordination Chemistry*, *64*(4), 725–741.

Liu, K., Liu, P., Liu, R., & Wu, X. (2015). Dual AO/EB staining to detect apoptosis in osteosarcoma cells compared with flow cytometry. *Medical Science Monitor Basic Research*, *21*, 15.

Ma, D., He, H., Leung, K., Chan, D. S., & Leung, C. (2013). Bioactive luminescent transition-metal complexes for biomedical applications. *Angewandte Chemie International Edition*, *52*(30), 7666–7682.

Marina, S. M. M. P. V. (2013). Noble metals in medicine: latest advances. *Drugs*, *24*, 131–139.

Mehta, P. D., Sengar, N. P. S., & Pathak, A. K. (2010). 2-Azetidinone–a new profile of various pharmacological activities. *European Journal of Medicinal Chemistry*, *45*(12), 5541–5560.

Nemati, L., Keypour, H., Shahabadi, N., Hadidi, S., & Gable, R. W. (2021). Synthesis, characterization and DNA interaction of a novel Pt (II) macroacyclic Schiff base complex containing the piperazine moiety and its cytotoxicity and molecular docking. *Journal of Molecular Liquids*, *337*, 116292.

Sathish Kumar, K., Chityala, V. K., Subhashini, N. J. P., & Prashanthi, Y. (2013). Synthesis, Characterization, and Biological and Cytotoxic Studies of Copper (II), Nickel (II), and Zinc (II) Binary Complexes of 3-Amino-5-methyl Isoxazole Schiff Base. *International Scholarly Research Notices*, *2013*.

Scattolin, T., Voloshkin, V. A., Visentin, F., & Nolan, S. P. (2021). A critical review of palladium organometallic anticancer agents. *Cell Reports Physical Science*, *2*(6), 100446.

Shahabadi, N., Kashanian, S., Mahdavi, M., & Sourinejad, N. (2011). DNA interaction and DNA cleavage studies of a new platinum (II) complex containing aliphatic and aromatic dinitrogen ligands. *Bioinorganic Chemistry and Applications*, *2011*.

Shahabadi, N., Kashanian, S., & Purfoulad, M. (2009). DNA interaction studies of a platinum (II) complex, PtCl2 (NN)(NN= 4, 7-dimethyl-1, 10-phenanthroline), using different instrumental methods. *Spectrochimica Acta Part A: Molecular and Biomolecular Spectroscopy*, *72*(4), 757–761.

Sharma, N. K., Ameta, R. K., & Singh, M. (2016). From synthesis to biological impact of Pd (II) complexes: synthesis, characterization, and antimicrobial and scavenging activity. *Biochemistry Research International*, *2016*.

Silva-Caldeira, P. P., Oliveira Junior, A. C. A. de, & Pereira-Maia, E. C. (2021). Photocytotoxic Activity of Ruthenium (II) Complexes with Phenanthroline-Hydrazone Ligands. *Molecules*, *26*(7), 2084.

Trondl, R., Heffeter, P., Kowol, C. R., Jakupec, M. A., Berger, W., & Keppler, B. K. (2014). NKP-1339, the first ruthenium-based anticancer drug on the edge to clinical application. *Chemical Science*, *5*(8), 2925–2932.

Uma Maheswari, P., Rajendiran, V., Palaniandavar, M., Parthasarathi, R., & Subramanian, V. (2005). Enantiopreferential DNA Binding:[{(5, 6-dmp) 2Ru} 2 (μ-bpm)] 4+ Induces a B-to-Z Conformational Change on DNA. *Bulletin of the Chemical Society of Japan*, *78*(5), 835–844.

Zeng, L., Li, Y., Li, T., Cao, W., Yi, Y., Geng, W., Sun, Z., & Xu, H. (2014). Selenium–platinum coordination compounds as novel anticancer drugs: selectively killing cancer cells via a reactive oxygen species (ROS)-mediated apoptosis route. *Chemistry–An Asian Journal*, *9*(8), 2295–2302.